The final published paper can be found at: https://doi.org/10.1109/EPTS61482.2024.10586732

A Review of Electromagnetic Simulation and Modelling Approaches for the Research on Axial Flux Synchronous Machines

Adrian Schäfer, Urs Pecha, Nejila Parspour
Institute of Electrical Energy Conversion (iew) of the University of Stuttgart
Stuttgart, Germany
adrian.schaefer@iew.uni-stuttgart.de

Achim Kampker, Henrik Born, Sebastian Hartmann
Chair of Production Engineering of E-Mobility Components (PEM) of RWTH Aachen University
Aachen, Germany
s.hartmann@pem.rwth-aachen.de

Jörg Franke, Marcel Baader, Roman Hahn
Institute for Factory Automation and Production Systems (FAPS) of the FAU Erlangen-Nürnberg
Nürnberg, Germany
marcel.baader@faps.fau.de

***Abstract*— Extensive electromagnetic (EMAG) studies are necessary to fully realize the potential of axial flux machines (AFMs). However, the disc-shaped air gap and the complex three-dimensional path of magnetic flux pose challenges in modelling AFMs compared to conventional radial flux machines. This study reviews current research on EMAG modelling and simulation of AFMs, highlighting the need for tools that address AFM-specific effects. Existing approaches are analysed based on the requirements composed by fundamental objectives of EMAG simulations and AFM-specific effects, revealing limitations in flexibility and the ability to capture emerging trends in the field of AFMs. While computationally expensive 3D finite element analysis (FEA) offers comprehensive flexibility in EMAG modelling, it lacks efficiency to carry out extensive studies on such trends. Therefore, there is a need to either further accelerate 3D FEA or to increase the flexibility of existing alternatives to facilitate and thereby promote research in the field of AFM and other 3D flux machines. While the integration of some production-specific effects, such as manufacturing tolerances, already is investigated for EMAG simulations of AFMs the future research on the early estimation of manufacturability based on EMAG simulations is crucial for evaluating designs and anticipating manufacturing influences.**

Keywords—axial flux machine, electromagnetic simulation, literature review, multi-domain, manufacturing effects

I. Introduction

Due to the potential of high torque density and efficiency as well as the possibility of modularisation and extension, the axial flux machine (AFM) is increasingly the focus of industry and research [1], [2]. In contrast to the radial flux machine (RFM), which has already been extensively investigated, there is still a need for further research into the AFM. Different topologies and designs of AFMs promise various advantages but also challenges [3], [4]. In addition to the construction and measurement of prototypes, computer-based modelling and simulation play an important role due to the significantly shortened feedback loop. This enables the efficient comparison of different topologies, designs, geometries and materials, the identification of sensitivities of these parameters, and the further enhancement of the overall performance of this type of machine. Electromagnetic (EMAG) simulation is at the centre of the simulative analysis of electrical machines. Similar to the transverse flux machine [5], the magnetic flux in the AFM is formed in three-dimensional space. In contrast to the RFM, where the magnetic flux is mainly restricted to a 2D plane, the electromagnetic simulation of the AFM is therefore significantly more challenging [6], [7]. As with the machine type of the AFM itself, different concepts and approaches have also been presented for its EMAG simulation and no method has yet been finally established to solve the conflict of objectives between efficient computing time, accuracy, flexibility, modelling detail and diversity of the target variables. Consequently, an overview and analysis of existing simulation methods is presented below, based on the structure of the AFM and its special effects. This analysis identifies potential gaps and research opportunities in the field of EMAG simulation of AFMs.

II. Method

An initial search is conducted as the starting point for the literature study. In order to obtain the broadest possible picture and publications from different institutions and publishers, "Google Scholar" is chosen as the search engine. In this search, the titles of scientific publications are checked for the search term shown in Fig. 1 which is composed of multiple parts that are linked via logical operators. The first two blocks ensure the focus on AFMs, while the last block is responsible for focusing on modelling and simulation methods. Patents are excluded from the search, as there is no focus on the simulation methodology. Furthermore, the articles are filtered manually to exclude false positive results that do not deal with the modelling and simulation of AFMs. At the same time, articles on AFMs as an induction machines are also filtered out, as the functional principle is different and the focus here is on machines that can be operated as synchronous machines.

In the first phase, based on the search term described in Fig. 1, articles were identified that deal with the development, validation or extension of simulation methods for AFMs, but also articles that exclusively describe the application of simulation methods, such as 3D finite element analysis (FEA), without focusing on the methodology. In order to enhance the focus on the approaches of EMAG modelling and simulation of AFMs, further articles on the method development of EMAG AFM simulations are identified in the second phase through citation links to the articles of the first phase. The result from the first and second phases is a literature collection of 85 categorised articles. These articles are presented in the

following in the form of distribution diagrams for different topics.

"axial flux" **OR** "axial field"

AND

"motor" **OR** "machine"

AND

"investigation" **OR** "examination" **OR** "analysis" **OR** "model" **OR** "simulation" **OR** "study" **OR** "analytic" **OR** "fea" **OR** "fem" **OR** "finite element" **OR** "magnetic equivalent circuit" **OR** "subdomain" **OR** "fourier"

Fig. 1. Search term for first literature acquisition

In addition to the EMAG simulation methodology for AFMs, an overview of possible designs of AFMs is required at the beginning, as the requirements for the simulation methods in this article are partly derived on the basis of the structure of the AFM. For this reason, overview papers on the design of AFMs are reviewed in an additional step and supplemented with related articles.

III. Overview of AFM Topologies and Designs

For the design analysis of the AFM, the seven overviews [8], [3], [9], [4], [10], [11] and [12] were analysed. The articles [9], [11] and [12] summarise the entire topology structure in a single diagram. Instead, in this work Fig. 2 provides an overview of the main topologies, which is detailed in Fig. 3 and Fig. 4 by subcategories for the stator and rotor design respectively. Overall, this enables a higher level of variety in the description of possible AFM topologies and designs. By combining a topology from Fig. 2 with specific choices for the stator and rotor design in Fig. 3 and Fig. 4 an overall design is generated. For instance, the topology of single stator double rotor (SSDR) with a pole orientation of north/ south, a core based and slotted but yokeless stator with concentrated ring windings as well as core based but slotless rotors with surface permanent magnets (PMs) leads to the well-known yokeless and segmented armature (YASA) design [13].

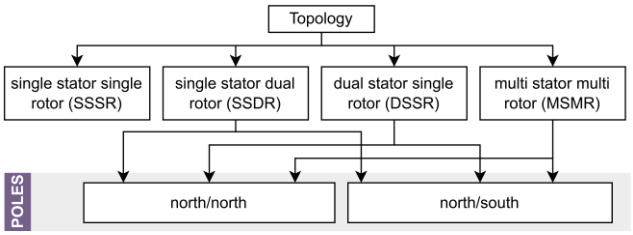

Fig. 2. Topologies of AFMs.

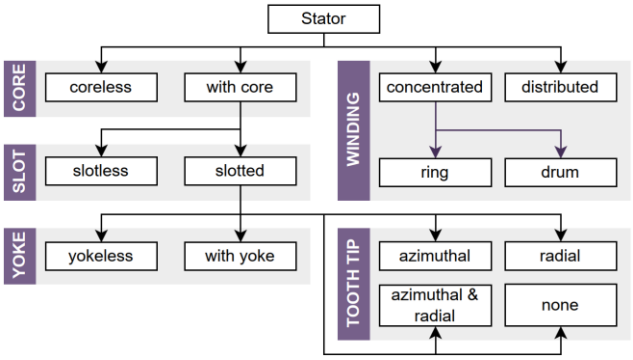

Fig. 3. Categories of stator design.

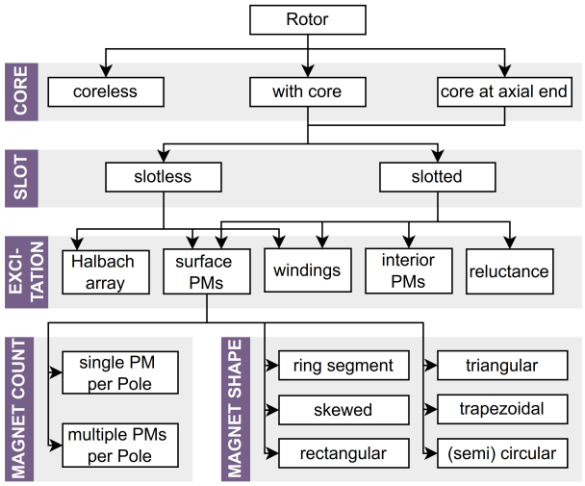

Fig. 4. Categories of rotor design.

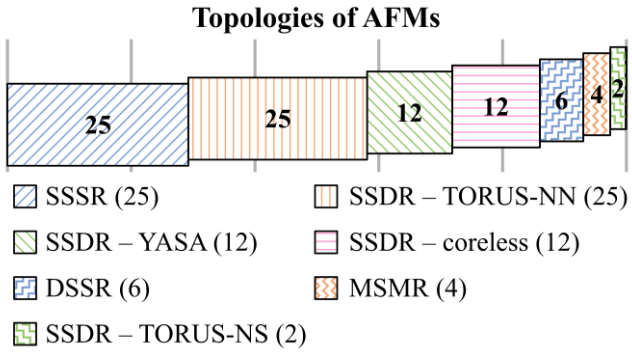

Fig. 5. Distribution of topologies in the EMAG simulation articles.

Changing the pole orientation to the north/ north orientation, the winding to a ring winding and adding a yoke leads to the so-called TORUS-NN design. As being illustrated in Fig. 5 both aforementioned design variants are represented extensively in the literature collection. The SSDR topology is therefore the most prevalent topology in the literature, followed by the SSSR topology.

As a design feature which is not included in the diagrams of [9], [11] and [12] the tooth tip design of stators with core and slots is included in Fig. 3 with the label "tooth tip". This design feature is explained in Fig. 6 where the different versions are shown for a half section of an YASA stator segment in a 3D section view and a front view respectively. The different forms of this feature are derived by analysing the overview papers and the reviewed literature. While the configuration without shoe is the most common, according to Fig. 7, the azimuthal tooth tip is widely used as well. This is because, both of these configurations come with less challenges in manufacturing the soft magnetic components as laminated steel cores [14], [15], [16], [17], [18] and also in the EMAG simulations, because the magnetic field is forced into 2D cylinder shell surfaces, thereby mainly behaving like a 2D flux machine [15], [18], [19], [20], [21], [22]. However, using a basic equation for the torque production of AFMs the benefit of radial tooth tips becomes evident. Based on [3] and [23] the average torque of an AFM is

$$T = B_{\mathrm{ag,avg}}\, m\, I\, N\, k_{\mathrm{w}}\, (R^2_{\mathrm{ag,out}} - R^2_{\mathrm{ag,in}}) \qquad (1)$$

where $B_{\mathrm{ag,avg}}$ is the average flux density in the air gap, m is the number of phases, N is the number of windings per phase, k_{w} is the winding factor and I is the rms phase current. $R_{\mathrm{ag,in}}$

and $R_{ag,out}$ are the inner and outer radii of the air gap zone respectively. The radial tooth tip increases $R_{ag,out}$ and decreases $R_{ag,in}$ while the outer dimensions remain constant, as these are defined by the inner and outer radii of the coils. Therefore, the radial tooth tips increase the torque output of the machine with a quadratic effect without changing the outer dimensions, thereby increasing the volumetric torque density. For this reason, tooth tip designs with a radial shoe as in the second column of Fig. 6 are of importance for the research on AFMs although such designs are underrepresented in the literature collection as is shown in Fig. 7. Nevertheless, in [1], [24], [25], [26] AFMs with radial tooth tips are investigated whereas in [27], [28], [29] and [30] the combination of radial and azimuthal tooth tips are shown.

In summary, the diagrams in this section expand the classifications from existing reviews by screening additional articles on the EMAG simulation methods of AFMs, thereby building the basis to evaluate special effects occurring in the AFM compared to the RFM.

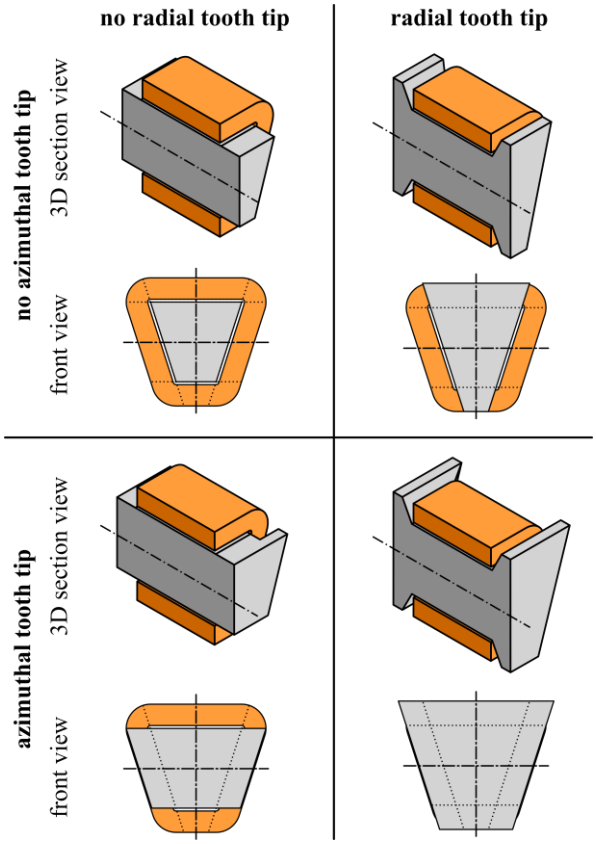

Fig. 6. Possible shapes of the stators tooth tip.

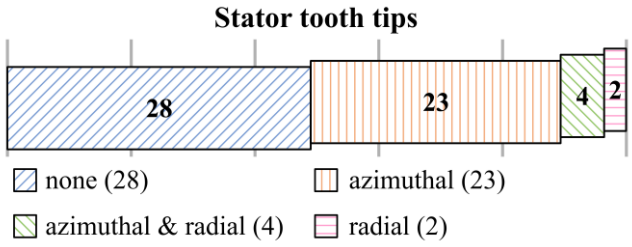

Fig. 7. Different forms of stator tooth tips.

IV. Special Effects for EMAG Models of AFMs

Due to the different shape of the air gap, the AFM has different magnetic flux paths compared to the RFM. This leads to effects that have a greater influence in the EMAG simulation of AFMs than in the simulation of RFMs. These effects are illustrated for AFMs with core in Fig. 8 and for AFMs without stator core in Fig. 9. Both figures show a half pole and a half coil of an exemplary AFM with simplified flux paths. The magnetic fields along the active length of an RFM are often neglected for simulation. With the AFM, however, the active length is orientated in the radial direction of the machine and is therefore comparatively short. For this reason, edge effects have a decisive influence on the magnetic field. The “radial leakage” effect, the “radially varying (air gap) field” effect and the “end winding effect” from Fig. 8 and Fig. 9 can mainly be attributed to the shorter active length and the associated end effects as well as the radial change in the magnetic circuit due to the change of circumference. However, as explained in the previous section, AFM designs can also include radial changes in geometries, such as special magnet, core or coil shapes. These design variations are complemented by radial and azimuthal tooth tips as well as radial diameter differences (“radial overhangs”) between the rotor and stator. The design differences have a direct influence on the EMAG conditions of the AFM and lead to further indirect effects. The saturation in the core material can vary radially ("radially varying saturation" effect). Radial notches in the core material lead to locally highly saturated zones ("radial notches" effect). Radial tooth tips in particular lead to radial magnetic field directions occurring in the cores, which cannot be neglected ("radial field direction" effect).

The effects mentioned here can be understood as requirements for the EMAG modelling and simulation methods of AFMs. The more of these effects can be replicated by a simulation method, the more generalised the corresponding approach can be applied to different types of AFMs and the better the suitability of the approach for comparisons between different AFM types.

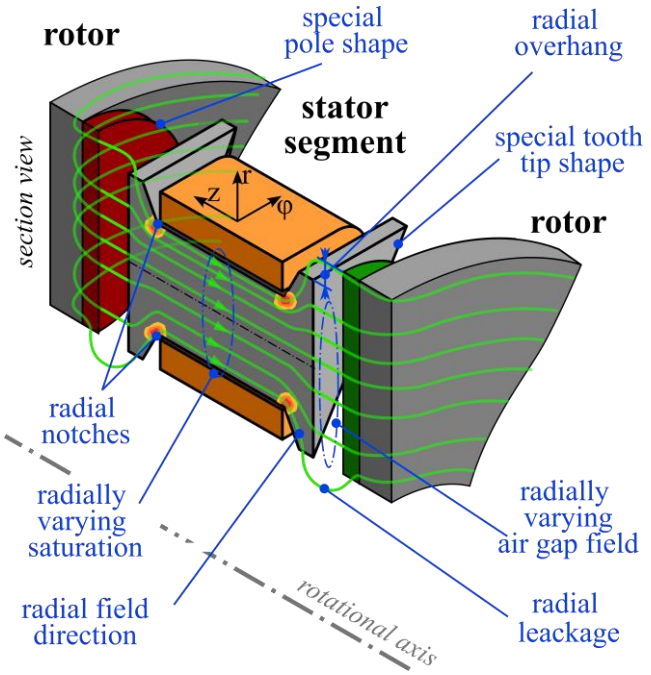

Fig. 8. Special effects in AFMs with core demonstrated on half stator segment and half rotor pole of an YASA AFM.

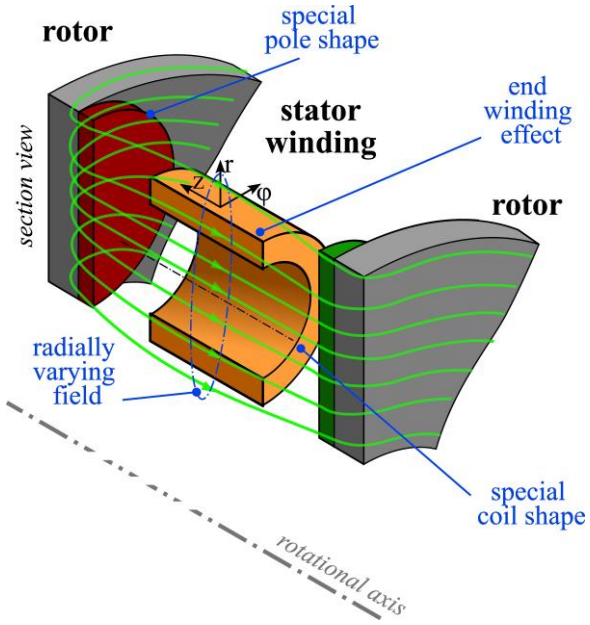

Fig. 9. Special effects in a coreless AFM demonstrated on half stator coil and half rotor pole.

V. Target Quantities of EMAG Simulations

EMAG simulations are executed in order to obtain certain target quantities of the electrical machine that characterise its behaviour. The resulting distribution of target quantities from the literature collection is shown in Fig. 11. The back electromotive force (back-EMF) as the most represented target describes the AFM from the electrical domain together with the coil inductances. On the other hand, the torque as the second most represented target and the torque ripple describe the interface to the mechanically connected systems. In addition, acting forces on the stator, the rotor or single subcomponents build another interface to a more detailed mechanical investigation of the AFM. Finally, the internal behaviour of the AFM is described by loss quantities and the magnetic air gap flux density. The latter enables more detailed information about the magnetic field solution, compared to other quantities like torque or back-EMF. The air gap flux density is therefore a popular method for comparing and validating different simulation methods and precisely identifying deviations. Another important target quantity is the opposing magnetic field in the PM in order to examine an operating point for demagnetisation. However, this target is not found in the literature collection.

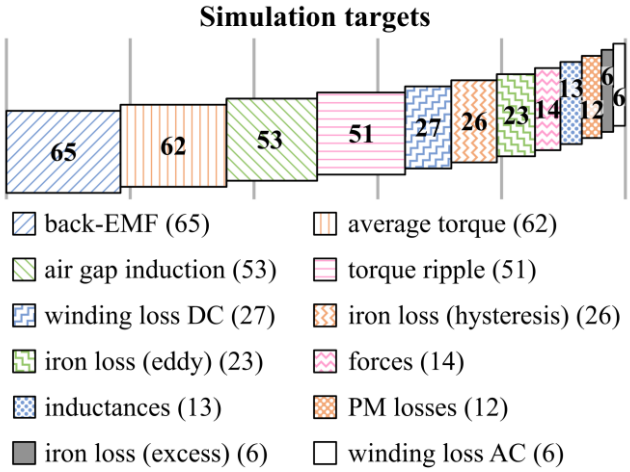

Fig. 10. Distribution of the most frequent simulation result quantities.

A. Torque Calculation

There are four torque calculation methods which is illustrated in Fig. 11. The Maxwell stress tensor (MST) can be derived from Lorentz force law and is used to calculate the torque based on the air gap flux densities in axial and azimuthal direction [30], [31]. A more robust extension to the MST for numerical simulation is the Arkkio method [30], [32] which is also labelled with MST in this work. The torque calculation method based on the conservation of electrical energy is applied in [33], [34] and [35]. With this approach, the electrical power is calculated on the basis of the back-EMF and the phase current. By dividing this power by the angular velocity, the torque is calculated directly. This method generally is only suitable for calculating the average torque. Instead, the Lorentz force utilized in [22], [36], [37] can be used to calculate instantaneous torque values based on coil-related variables. However, when it comes to the torque ripple only the harmonic torque components of the armature winding are considered and the cogging torque caused by the PM induced rotor field is neglected by the calculation based on Lorentz force. The methods mentioned so far can be applied as post-processing to an EMAG field problem that has already been solved. However, for the virtual energy method, the partial derivative of the magnetic co-energy according to the motion variable must be calculated during the solution process. Therefore, although being able to calculate all torque and torque ripple components this method is usually only used in the context of magnetic equivalent circuits (MECs), since the co-energy calculation is comparatively simple there [38], [39], [40].

B. Force Calculation

Due to the comparatively large outer diameter of the AFM, the axial forces acting between the stator and rotor lead to the deformation of the rotor, which can close the air gap and thus damage the machine [41]. For this reason, analysing the axial forces is of great importance. Nevertheless, the target of force calculation appears to be underrepresented in the literature with 14 articles. The force between the stator and rotor can be calculated using the MST and the air gap flux density [41]. The literature mainly analyses static maximum forces [42]. Only [14], [43] and [44] carry out dynamic analyses based on the harmonic components of the forces. In the literature collection, there is no feedback of the mechanical deformations into the EMAG simulation to analyse the feedback effects. Moreover, [44] comes to the conclusion that the force calculation using the magnetic air gap flux density is not sufficient for a detailed mechanical investigation of the vibration, but that the surface forces of the components must be used instead.

C. Loss Calculation

As with the RFM, the losses in the ferromagnetic core can be calculated in a post-processing step after solving the field problem with the loss formulae according to Bertotti [45] or Steinmetz [46] or with loss maps [15], [16]. The dynamic effect of the loss mechanisms on the magnetic field is neglected in this case. But such influences have already been investigated for the AFM in individual articles [47], [48].

Evaluating the distribution in Fig. 10, the DC winding losses are mainly considered as the only winding losses and the AC winding losses are strongly underrepresented.

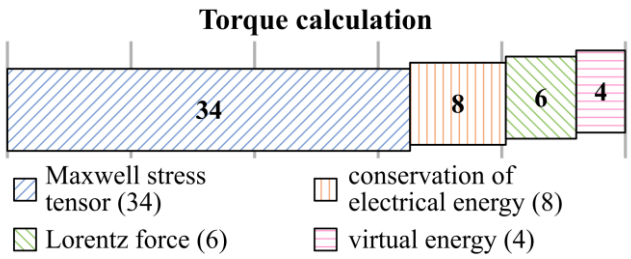

Fig. 11. Distribution of torque calculation methods.

There already exist studies on the AC winding losses in AFMs by [49] and [50] as well as a loss model for the AC winding losses for AFMs with coreless stator [51], which indicate the significance of the AC winding losses. Therefore, further investigations as well as the development of further loss models or calculation methodologies of different types of AFMs are necessary. Calculation methodologies could, for example, be based on the AC loss calculation in the 2D FEA, as demonstrated in [49]. In order to increase the accuracy of AFM loss and efficiency calculations, it is important that the calculation of AC copper losses is widely used in AFM research.

Compared to the iron losses, the PM losses are also underrepresented in Fig. 10. The PM losses are due to the eddy currents in the PMs. In addition to the losses, the eddy currents form a magnetic reaction field that influences the dynamic behaviour of the fields and the machine. In addition to the solution of the transient Maxwell equations in 3D space [49], [52], various approaches already exist for calculating the eddy current losses of AFMs with and without taking the reaction field into account [53], [54], [55]. The approaches are generally based on a model of the electric fields that form within the PM in the plane orthogonal to the axis of rotation of the AFM.

VI. Spatial Dimensions of EMAG Simulations

As described in the previous chapter, the magnetic flux density is a decisive target variable for describing the magnetic field in electrical machines. The magnetic field can be formulated in one, two or three dimensions. Although in AFMs, as described in section IV, radial or 3D effects occur, for some types of AFMs the modelling of the magnetic field in one or two dimensions already leads to accurate results. The distribution between 1D, 2D and 3D simulation in the literature collection is given in Fig. 12. Especially 2D simulations are used as an alternative to 3D simulation. In the following, the transformation from the 3D design of an AFM into lower dimensions is described.

A. Slices

Since the stator, rotor and active air gap have an annular shape, the transformation into 2D space takes place along a cylindrical surface that is aligned coaxially to the axis of the machine and intersects the active area of the machine. This process is shown in the upper part of Fig. 13. The transformation to a lower dimension means that the radial effects from section IV are neglected. In order to reproduce some of these effects nevertheless, it is possible to model the 3D space not in one but in several 2D spaces. This is the fundamental idea behind the multi-slice approach, which is often referred to as the quasi 3D method and is illustrated in the lower part of Fig. 12. Although with the multi-slice method the magnetic field is solved at different radii, it still has no radial components due to the alignment of the slices.

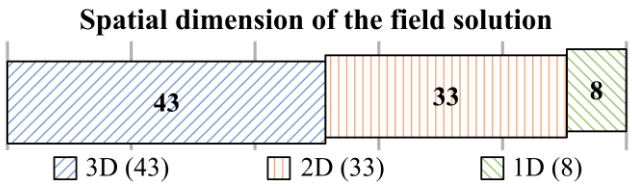

Fig. 12. Spatial dimension of the simulation approaches considered.

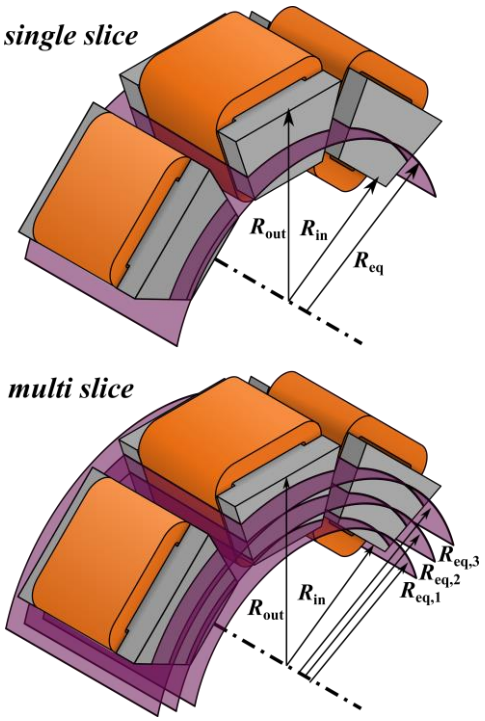

Fig. 13. Single and multi slice 2D simulation concept demonstrated on the periodical stator section of an YASA AFM.

Therefore, although the multi-slice approach is capable of modelling effects depending on the radius, such as the radial change in shape of subcomponents or the radial change in field distribution and the radial change in saturation of ferromagnetic components, effects caused by a radial field direction are neglected. For this reason, the effect of radial tooth tips, radial notch effects and radial end effects as well as a radial overhang between rotor and stator are not modelled with the multi-slice method.

Regarding the radial distribution of the slices most approaches of the multi-slice method utilize an equal distribution, however there are exceptions. In [16] and [18] thinner slices are used towards the radial ends of zones, because tests showed higher accuracy with this arrangement. This could indicate that there occurs a border effect for the inner and outer most slices. To overcome such an effect in [56] slices are always placed at the inner and outer most radial position and interpolation is used to get results for arbitrary radii.

B. Equivalent Radius

The equivalent radius defines the position of the cylindric cutting surface from which the individual slice simulation models are derived. In about 73% of the 2D modelling methods the average radius of the selected 3D ring section is used. No definition of the equivalent radius is given in 17% of the articles, whereas in [27], [38] and [57] other definitions of the equivalent radius like the mean square average or an approach based on the magnetic energy are used.

C. Transformations

Finally, the target space of the 3D to 2D transformation is regarded. According to Fig. 14, the transformation from the cylindrical surface of the rotational AFM to a flat surface with cartesian coordinates of an equivalent linear machine is the most common. This transformation is employed, particularly in the context of 2D FEA, because there is no possibility of executing a 2D EMAG analysis on a cylindrical surface using the majority of numerical simulation software. The rotational AFM repeats periodically and infinitely along the azimuthal direction. However, for a linear machine there is an end in the direction of movement. Therefore, if possible the correct periodic conditions must be applied at the azimuthal end of the simulation space [30]. Otherwise, workarounds like [19] have to be implemented to avoid azimuthal end effects from the linear machine affecting the results. If another transformation is used this effect can be avoided as well. Instead of transforming to a linear machine the AFM slice can be transformed to either an inner or outer rotor RFM. This has the advantage that the extensive simulation methodology of the RFM can be applied to the AFM, but with this transformation the dimensions of the components are distorted and scaled with increasing distance from the air gap. Furthermore, some MSMR AFMs are difficult to simulate with this approach. For further details of this transformation, it is referred to [19] and [58]. Finally, the last approach is to not transform the slices and solve the magnetic field directly on the cylindrical surface. This approach is associated with the least transformation effort [59], [60].

VII. Common Simulation Approaches

In this section the major EMAG simulation approaches based on the literature collection are described with respect to the criteria and requirements derived in the previous sections.

A. Analytical and Semi Analytical Methods

1) Fourier-based Methods

a) One Dimensional Fourier Air Gap Models

For simple initial estimates of an AFM, it is possible to model the air gap field of the machine one-dimensionally with a Fourier series at the centre radius. Consequently, radial effects are neglected. In some cases, the Fourier series is derived directly from the magnet arrangement using simplified assumptions, as in [34], [61] and [62]. Alternatively, a Fourier series for the magnetomotive force at the air gap and a second Fourier series for the variable permeance of the air gap are established and the distribution of the air gap flux density is derived by multiplication [63], [64]. This also allows cogging torque to be accounted for. Other target variables such as the back-EMF can be derived on the basis of the winding function theory [62]. Soft magnetic components are modelled with infinite permeability, without saturation and without losses [62]. The method is therefore only suitable for basic estimates, especially if a very short calculation time is required.

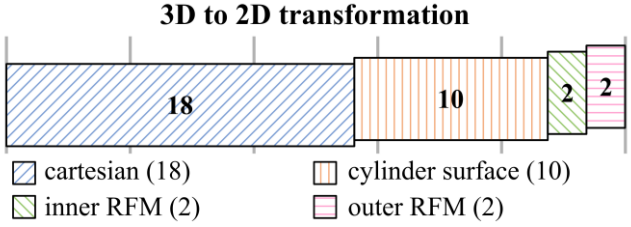

Fig. 14. Target space of 3D to 2D transformations.

b) Magnetic Scalar Potential Air Gap Models

In this approach, only the unloaded PM excited field of the rotor between two magnetically infinitely conductive discs is considered as the field solution. This approach is therefore only suitable for coreless or slotless AFMs. Due to the absence of free currents, the magnetic scalar potential is used as a solution variable and thus the Poisson equation and partially also the Laplace equation are formulated for the regions of the PMs and the air. The magnetisation effect of the PMs is represented by Fourier series and the relative permeability of the PMs is neglected. The air-gap magnetic field is solved either in two dimensions for the average φ-z plane of the air-gap [35], [43], [65], [66] or in the three-dimensional r-φ-z volume [36], [37], [60], [67], [68] of the air-gap. The 2D solutions often refer to solutions for RFMs as for example to [69]. In the 3D solutions, the radial variation of the flux density and the radial end winding effects are considered. In order to be able to map these effects with the 2D solution, a 3D solution is constructed from the 2D solution in [43] using a radial correction function. An alternative is the usage of multiple 2D slices as in [65]. Examining the geometric shapes, for the 2D as well as the 3D solutions mainly the standard ring segment shapes are represented. Exceptions to this observation are the Halbach array in [37] and the circular coil in [67]. To derive the electrical simulation targets like back-EMF from the field solution, the flux density distribution is integrated over the coil area and the time derivative is calculated [43], [66]. As another simulation target the torque can be calculated with the Lorentz force [36] or by using the conservation of electrical energy method [35]. Losses like AC winding loss, iron loss or PM losses are not considered in the articles on this method. In summary, this method can be used to generate 3D air gap fields for coreless or slotless AFMs with modest effort, but it lacks the flexibility of geometric shapes, the consideration of saturation effects and loss considerations.

c) Magnetic Vector Potential Models

The methods presented previously based on Fourier series can neither model free currents nor ferromagnetic material behaviour. For this reason, methods have been developed that use the magnetic vector potential as a solution variable, which allows the effect of currents to be considered. In these approaches, however, the magnetic field is solved exclusively in a 2D plane, which means that the vector potential has a single component [70]. Consequently, the multi-slice method is necessary to account for radial effects of the AFM. A complete reproduction of all the effects listed in Section IV is therefore not possible. Nevertheless, the models presented here offer advantages when modelling slotting effects, materials and losses. Although losses such as eddy currents are neglected, approximation methods such as the loss calculation based on Steinmetz can be used on the basis of the field distribution within the material [20]. The material properties, magnetisation effect and current effect are defined either by defining individual zones or as Fourier series within a layer [71]. The first method is referred to as the subdomain model [58], [72]. In this work the second method is referred to as layer model [22], [70], [73]. The layer models presented in [21] and [73] define the permeability in a layer by a Fourier series thereby being able to account for a finite value of the relative permeability of iron. Moreover, an iterative process is utilized in both of these articles to solve for non-linear saturation of the iron. As the methods presented in this subsection model the on-load magnetic field MST is used to

calculate torque, torque ripple and forces [71]. The back-EMF is derived by calculating the time derivative of the integral of the flux density over a coil pitch span [73]. Overall, the features of this method are more comprehensive than the other methods based on Fourier series, but the flexibility in the choice of geometry remains limited and not all radial effects of the AFM can be modelled. Furthermore, there is no methodology for a detailed and accurate incorporation of losses and their dynamic effects.

2) Magnetic Equivalent Circuit

The MEC approach uses circuit theory to model and solve the magnetic field. The magnetic circuit can be weakly or strongly linked to the geometry of the machine, leading to simple [74], [75] or very complex [15], [48] grid-like circuits, which in extreme cases are similar to finite element meshes. In most cases, however, the circuit has a medium complexity comparable to [76], [77], [78] or [79], whereby nodes of the circuit are created for individual sub-zones of the machine and adjacent nodes are linked via wires. The magnetic conductivity of the materials and media are represented by lumped resistors (reluctances) and the magnetomotive force of magnets and coils by voltage sources. Because the equivalence between the real geometry and the circuit is flexibly definable also the dimensions and the resolution of the total circuit can be variable within one model. Furthermore, if the reluctances are defined as parts of ring segments the MEC can directly describe the ring shape of the AFM as a 2D circuit, as multi-slice 2D circuits or as a 3D circuit without a transformation to a linear equivalent machine [59]. Regarding ferromagnetic material properties of the soft magnetic cores the MEC approach enables the utilization of nonlinear reluctances which can be solved comparably easy due to the circuit theory. Moreover, even dynamic behaviour can be modelled using inductances in the magnetic circuit. These magnetic inductances can replicate eddy current or hysteresis effects, that can be solved dynamically in the MEC thereby directly considering the effect of reaction fields [38]. Additionally an electrical circuit can be introduced similar to [55], [80] or [81] which is able to model the eddy current effect based on the geometry of a cross section and which is linked to the MEC. In summary, there exists great potential of the MEC to dynamically and accurately model the soft magnetic material behaviour. In contrast, the modelling of low-permeability zones such as air or PMs with MECs is a greater challenge than, for example, with Fourier-based analytical models. With different approaches, such as the use of flux tubes [24], [39], [79], conformal mapping [78], or high-resolution MEC networks [82], [83], these zones can still be modelled with high accuracy. Nevertheless, for the first two approaches, prior knowledge of the field paths is required and the latter increases the computational effort. Finally the relative movement between stator and rotor poses another challenge, which is solved by step-wise or zone-wise reconnecting wires [24], [79], [83], steadily changing the values of the air gap reluctances [24], [79] or interpolating on a sliding interface [82]. Alternatively the circuit stays constant while the rotor circuit elements change their properties to simulate movement [15].

To summarise, MECs are capable of considering all special effects, calculating target variables and offering extensive functions, e.g. dynamic material behaviour. However, the different options for modelling the air gap and movement should be compared and evaluated in a standardised manner in order to identify the approach with the objectively highest accuracy and calculation efficiency.

B. Numerical Simulation

1) 2D FEA

With 2D FEA all target quantities from section V except for the end winding components of the AC winding losses and the exact eddy currents can be calculated. As in [49] only the radially oriented conductors can be modelled in the cylinder surface for the transient winding loss calculation. However, the magnetic field at the radial ends is not guaranteed to be similar to the field occurring in the windings between two adjacent stator teeth. This can lead to inaccuracies in the winding loss calculation. To be able to model the eddy currents especially in the solid and conductive PMs additional models like [54] or [63] must be used and linked with the magnetic simulation. In addition to the target quantities, the capability of modelling the special effects of the AFM for different 2D FEA approaches is analysed.

First the single slice 2D FEA using analytical extensions like [33] is investigated. Although saturation is considered in the 2D model, the radial change of saturation is not. Despite the radial change of the outer contours of the active components, such as the PMs, can be modelled with this method, it is not possible to include the radial tooth tips and the associated radial field components and radial notch effects. Furthermore, the radial end-effects and the radial overhang are not considered as well. Next, the fundamental multi-slice 2D FEA which is described in [84] and [85] is analysed. While mainly having the same properties as the single slice 2D FEA with analytical extension different saturation levels can be modelled radially due to the discrete slices. However, because the slices are not linked, radial field components, radial notch effects and radial end effects are not modelled. Therefore, an extension is proposed in [86] to consider radial end effects based on an analytical function similar to the functions used in the section of analytical models. Another extension is suggested in [56] where interpolation between radial adjacent slices is used to receive an steady field result in the radial direction. Finally there is an additional extension by the company VEPCO Technologies which provides information about a multi-slice EMAG simulation approach for the software MotorXP-AFM [87]. In addition to the cylindrical multi slices another cutting plane in the r-z-plane in the centre of a stator segment is applied. In this plane radial field components are modelled allowing the magnetic flux to enter radial tooth tips, to build up leakage paths at the radial ends and to consider the radial notch effects. Such approaches enable the extended applicability of the 2D multi-slice FEA methodology, which increasingly imitates the full functionality of 3D FEA with less computational effort, making the methodology a serious alternative.

2) 3D FEA

3D FEA is by far the most widely used EMAG simulation method for AFMs. About 45% of the articles of the collection use 3D FEA as the main method and another 45% use 3D FEA to verify other simulation methods. This is because 3D FEA is able to model all special effects of the AFM from section IV and retrieve all targets quantities from section V. The computational expense is still the major drawback of this method, especially when all effects and targets are solved for in a time stepping dynamic simulation. While most of the 3D FEAs use the magnetic vector potential as dependent variable, there exist approaches to significantly reduce simulation time

by using the magnetic scalar potential not only for the magnet regions but also for the coil regions as demonstrated in [30], [88] and [89]. For this approach, however, all time dependent effects and losses are to be calculated with other methods in a postprocessing step. Another approach to accelerate 3D FEA is the field reconstruction method. The geometrical symmetry and periodicity as well as the time based periodicity of the AFM are used to replicate the distribution of the magnetic field from a few finite element simulation steps [90], [91]. By applying both approaches mentioned an acceleration by one or two magnitudes is possible, thereby enhancing the applicability of the 3D FEA for AFMs.

VIII. Interfaces To Manufacturing Processes And Material Science

In this section the influences of manufacturing process and materials on the EMAG simulation of AFMs are lined out.

A. Manufacturing Processes

The literature collection shows that research is currently mainly investigating simplified nominal AFM designs. In reality, however, the production of components is subject to dimensional and shape deviations that lead to positional deviations during assembly. The adhesives or fasteners used can also lead to further positional deviations. This can lead to gaps between the active magnetic components that impair the behaviour of the AFM. However, the literature collection does not contain any studies on the effects of gaps between active components. Furthermore, chamfers or radii are present at the edges of the active components due to the manufacturing influences described. Although the influences of these effects are investigated in [30] and [64], they are not the focus of the analysis there. As the modelling and simulation of detailed geometries is complex for all simulation methods, the coils of the AFM are also often simplified. Only in 6 articles of the literature collection individual conductors are modelled, in 62 articles the coil is represented by a simplified geometry. In the remaining articles, only the PM field was considered and the coil was therefore not modelled. As already mentioned in the subsection “Loss Calculation”, the modelling of the conductors has a decisive influence on the AC winding losses of the AFM. For an accurate loss estimation, the modelling of individual conductors or the use of accurate approximation models is therefore crucial. As pointed out in the subsection “Force Calculation” the axial forces between rotor and stator can significantly influence the operation of an AFM. For this reason, various deviation analyses of the alignment errors of the rotor and stator have already been carried out. Specifically, the radial axis offset [58], the angular deviation of the rotor axis and a single rotor disc [52], [58] and the axial deviation between the stator and rotor [52], [75] were investigated. So initial findings already exist in the literature for these production-related deviations of the AFM.

B. Materials

For the EMAG simulation of AFM especially the electrical and magnetic conductors are important. As hard magnetic material in about 90% of the articles where an indication of the PM material is given, neodymium magnets (NdFeB) are used. In the literature collection by far the most used material for the windings of the AFM is solid copper wire. However, Litz wire [92], carbon nano tubes [93] and superconductors [57], [94], [95], [96] are represented as well. For Litz wire and superconductors special loss models mentioned in the respective references must be used. Furthermore, the EMAG fields in superconductors are not solved with the magnetic vector potential but with a formulation based on either the magnetic field or the current vector potential [57]. These are the major changes required to implement these materials into the EMAG simulation.

With regard to the ferromagnetic components of the AFM, in the literature collection most frequently iron or electrical steel as solid materials are used in the rotor, followed by laminated electrical steel. In the stator, laminated electrical steel and soft magnetic composite (SMC) are most frequently used due to the larger influence of alternating fields. Because of the wide application of laminated electrical steel in the literature collection, the geometric diversity of the corresponding AFM designs is limited. Therefore, designs with radial tooth spacing of the stator teeth are also avoided. Instead, SMC offers more flexibility in the design of the core segments, but has unfavourable magnetic properties, such as a lower permeance and saturation flux density [97]. In the future, multi-material cores such as [98] or additively manufactured cores such as [99] that include thin gaps to prevent eddy currents could solve this conflict of objectives. For the EMAG simulation of the first approach, the modelling method must include an efficient implementation of low-permeability gaps in order to be able to simulate the interfaces between different materials. For the EMAG simulation of the additively manufactured core the modelling method either has to efficiently solve the magnetic field for the combination of thin low-permeability gaps and detailed core structures or an efficient and simplified substitute model must be developed. So, in future, there will be further new challenges and requirements for EMAG simulation methods.

IX. Conclusion

The main findings of this review are:

1. Radial tooth tips can increase the torque and power density but quasi 3D methods are currently not able to replicate all occurring effects of this feature.
2. AC winding and PM losses are underrepresented in the literature collection. Especially for AC winding losses further investigations and simplified models are needed.
3. Models based und Fourier-series still need further development to compete with MECs or FEA.
4. MEC models are flexible and scalable. Especially saturation and dynamic behaviour such as hysteresis and eddy current can be efficiently solved.
5. Additional r-z-slices that are coupled to the standard z-φ-slices could further improve multi-slice 2D FEA.
6. The field reconstruction method and the magnetic scalar potential significantly accelerate 3D FEA.
7. Not all relevant influences of production and materials on EMAG simulation have been analysed by research to date. New trends are creating new challenges, such as the simulation of fine additively manufactured structures.

These findings show additional requirements for future research on the EMAG modelling and simulation methods.

REFERENCES

[1] B. Zhang, T. Epskamp, M. Doppelbauer, and M. Gregor, "A comparison of the transverse, axial and radial flux PM synchronous motors for electric vehicle," in *2014 IEEE International Electric Vehicle Conference (IEVC 2014): Florence, Italy, 17 - 19 December 2014*, Florence, 2014, pp. 1–6.

[2] A. Echle, A. Neubauer, and N. Parspour, "Design and Comparison of Radial Flux and Axial Flux Brushless DC Motors for Power Tool Applications," in *Proceedings 2018 XIII International Conference on Electrical Machines (ICEM): Ramada Plaza Thraki, Alexandroupoli, Greece, 03-06 September, 2018*, Alexandroupoli, 2018, pp. 125–130.

[3] J. F. Gieras, R.-J. Wang, and M. J. Kamper, *Axial flux permanent magnet brushless machines*, 2nd ed. New York: Springer, 2008.

[4] A. Habib *et al.*, "A systematic review on current research and developments on coreless axial ‐ flux permanent ‐ magnet machines," *IET Electric Power Appl*, vol. 16, no. 10, pp. 1095–1116, 2022, doi: 10.1049/elp2.12218.

[5] B. Kaiser and N. Parspour, "Transverse Flux Machine—A Review," *IEEE Access*, vol. 10, pp. 18395–18419, 2022, doi: 10.1109/ACCESS.2022.3150905.

[6] J.-W. Jung, H.-I. Park, J.-P. Hong, and B.-H. Lee, "A Novel Approach for 2-D Electromagnetic Field Analysis of Surface Mounted Permanent Magnet Synchronous Motor Taking Into Account Axial End Leakage Flux," *IEEE Trans. Magn.*, vol. 53, no. 11, pp. 1–4, 2017, doi: 10.1109/TMAG.2017.2706729.

[7] T. F. Chan, W. Wang, and L. L. Lai, "Performance of an Axial-Flux Permanent Magnet Synchronous Generator From 3-D Finite-Element Analysis," *IEEE Trans. Energy Convers.*, vol. 25, no. 3, pp. 669–676, 2010, doi: 10.1109/TEC.2010.2042057.

[8] S. Amin, S. Khan, and S. S. Hussain Bukhari, "A Comprehensive Review on Axial Flux Machines and Its Applications," in *2019 2nd International Conference on Computing, Mathematics and Engineering Technologies (iCoMET)*, Sukkur, Pakistan, 2019, pp. 1–7.

[9] F. Giulii Capponi, G. de Donato, and F. Caricchi, "Recent Advances in Axial-Flux Permanent-Magnet Machine Technology," *IEEE Trans. on Ind. Applicat.*, vol. 48, no. 6, pp. 2190–2205, 2012, doi: 10.1109/tia.2012.2226854.

[10] Z. Hao, Y. Ma, P. Wang, G. Luo, and Y. Chen, "A Review of Axial-Flux Permanent-Magnet Motors: Topological Structures, Design, Optimization and Control Techniques," *Machines*, vol. 10, no. 12, p. 1178, 2022, doi: 10.3390/machines10121178.

[11] S. Kahourzade, A. Mahmoudi, H. W. Ping, and M. N. Uddin, "A Comprehensive Review of Axial-Flux Permanent-Magnet Machines," *Can. J. Electr. Comput. Eng.*, vol. 37, no. 1, pp. 19–33, 2014, doi: 10.1109/CJECE.2014.2309322.

[12] F. N. Nishanth, J. van Verdeghem, and E. L. Severson, "A Review of Axial Flux Permanent Magnet Machine Technology," *IEEE Trans. on Ind. Applicat.*, vol. 59, no. 4, pp. 3920–3933, 2023, doi: 10.1109/tia.2023.3258933.

[13] T. J. Woolmer and M. D. McCulloch, "Analysis of the Yokeless And Segmented Armature Machine," in *2007 IEEE International Electric Machines and Drives Conference: IEMDC] ; Antalya, Turkey, 3 - 5 May 2007*, Antalya, Turkey, 2007, pp. 704–708.

[14] A. Credo, M. Tursini, M. Villani, C. Di Lodovico, M. Orlando, and F. Frattari, "Axial Flux PM In-Wheel Motor for Electric Vehicles: 3D Multiphysics Analysis," *Energies*, vol. 14, no. 8, p. 2107, 2021, doi: 10.3390/en14082107.

[15] A. Hemeida *et al.*, "A Simple and Efficient Quasi-3D Magnetic Equivalent Circuit for Surface Axial Flux Permanent Magnet Synchronous Machines," *IEEE Trans. Ind. Electron.*, vol. 66, no. 11, pp. 8318–8333, 2019, doi: 10.1109/TIE.2018.2884212.

[16] D. Kowal, P. Sergeant, L. Dupre, and A. van den Bossche, "Comparison of Nonoriented and Grain-Oriented Material in an Axial Flux Permanent-Magnet Machine," *IEEE Trans. Magn.*, vol. 46, no. 2, pp. 279–285, 2010, doi: 10.1109/TMAG.2009.2032145.

[17] A. Mahmoudi, S. Kahourzade, N. A. Rahim, and W. P. Hew, "Design, Analysis, and Prototyping of an Axial-Flux Permanent Magnet Motor Based on Genetic Algorithm and Finite-Element Analysis," *IEEE Trans. Magn.*, vol. 49, no. 4, pp. 1479–1492, 2013, doi: 10.1109/tmag.2012.2228213.

[18] H. Vansompel, P. Sergeant, and L. Dupre, "Optimized Design Considering the Mass Influence of an Axial Flux Permanent-Magnet Synchronous Generator With Concentrated Pole Windings," *IEEE Trans. Magn.*, vol. 46, no. 12, pp. 4101–4107, 2010, doi: 10.1109/TMAG.2010.2070075.

[19] C. Corey, J. H. Kim, and B. Sarlioglu, "2-D Modeling and Experimental Testing of Single Rotor Dual Stator Axial-Flux Permanent Magnet Machines," in *ECCE 2019: IEEE Energy Conversion Congress & Expo : Baltimore, MD, Sept. 29-Oct. 3*, Baltimore, MD, USA, 2019, pp. 2996–3003.

[20] Y. Du, Y. Huang, B. Guo, F. Peng, and J. Dong, "Semianalytical Model of Multiphase Halbach Array Axial Flux Permanent-Magnet Motor Considering Magnetic Saturation," *IEEE Trans. Transp. Electrific.*, vol. 9, no. 2, pp. 2891–2901, 2023, doi: 10.1109/TTE.2022.3229051.

[21] B. Guo *et al.*, "Nonlinear Semianalytical Model for Axial Flux Permanent-Magnet Machine," *IEEE Trans. Ind. Electron.*, vol. 69, no. 10, pp. 9804–9816, 2022, doi: 10.1109/TIE.2022.3159952.

[22] J. Si, Y. Wei, R. Nie, J. Liang, C. Gan, and Y. Hu, "Analytical Modeling of Slotless Axial Flux Permanent Magnet Motor With Equidirectional Toroidal Winding," *IEEE Trans. Ind. Electron.*, vol. 70, no. 10, pp. 10420–10430, 2023, doi: 10.1109/tie.2022.3222612.

[23] M. Waldhof, A. Echle, and N. Parspour, "A Novel Drive Train Concept for Personalized Upper Body Exoskeletons with a Multiphase Axial Flux Machine," in *2019 IEEE International Electric Machines & Drives Conference (IEMDC)*, San Diego, CA, USA, 2019, pp. 2160–2166.

[24] P. Ojaghlu, A. Vahedi, and F. Totoonchian, "Magnetic equivalent circuit modelling of ring winding axial flux machine," *IET Electric Power Applications*, vol. 12, no. 3, pp. 293–300, 2018, doi: 10.1049/iet-epa.2017.0517.

[25] B. Zhang and M. Doppelbauer, "Iron Losses Calculation of an Axial Flux Machine Based on Three-Dimensional FEA Results Corresponding to One-Sixth Electrical Period," *IEEE Trans. Energy Convers.*, vol. 32, no. 3, pp. 1023–1030, 2017, doi: 10.1109/TEC.2017.2674304.

[26] B. Zhang, T. Seidler, R. Dierken, and M. Doppelbauer, "Development of a Yokeless and Segmented Armature Axial Flux Machine," *IEEE Trans. Ind. Electron.*, p. 1, 2015, doi: 10.1109/TIE.2015.2500194.

[27] J. S. Kim, J. H. Lee, J.-Y. Song, D.-W. Kim, Y.-J. Kim, and S.-Y. Jung, "Characteristics Analysis Method of Axial Flux Permanent Magnet Motor Based on 2-D Finite Element Analysis," *IEEE Trans. Magn.*, vol. 53, no. 6, pp. 1–4, 2017, doi: 10.1109/tmag.2017.2665484.

[28] S. S. Nair, S. Nalakath, and S. J. Dhinagar, "Design and analysis of axial flux permanent magnet BLDC motor for automotive applications," in *2011 IEEE International Electric Machines & Drives Conference (IEMDC 2011): Niagara Falls, Ontario, Canada, 15 - 18 May 2011*, Niagara Falls, ON, Canada, 2011, pp. 1615–1618.

[29] L. Xu, Y. Xu, and J. Gong, "Analysis and Optimization of Cogging Torque in Yokeless and Segmented Armature Axial-Flux Permanent-Magnet Machine With Soft Magnetic Composite Core," *IEEE Trans. Magn.*, vol. 54, no. 11, pp. 1–5, 2018, doi: 10.1109/TMAG.2018.2850317.

[30] A. Schäfer, U. Pecha, B. Kaiser, M. Schmid, and N. Parspour, "Accelerated 3D FEA of an Axial Flux Machine by Exclusively Using the Magnetic Scalar Potential," *Energies*, vol. 16, no. 18, p. 6596, 2023, doi: 10.3390/en16186596.

[31] P. Virtic, P. Pisek, M. Hadziselimovic, T. Marcic, and B. Stumberger, "Torque Analysis of an Axial Flux Permanent Magnet Synchronous Machine by Using Analytical Magnetic Field Calculation," *IEEE Trans. Magn.*, vol. 45, no. 3, pp. 1036–1039, 2009, doi: 10.1109/tmag.2009.2012566.

[32] A. Arkkio, *Analysis of induction motors based on the numerical solution of the magnetic field and circuit equations*. Zugl.: Otaniemi, Helsinki Univ. of Technology, Diss., 1987. Helsinki: Finnish Acad. of Technology, 1987.

[33] A. Egea, G. Almandoz, J. Poza, G. Ugalde, and A. J. Escalada, "Axial-Flux-Machine Modeling With the Combination of FEM-2-D and Analytical Tools," *IEEE Trans. on Ind. Applicat.*, vol. 48, no. 4, pp. 1318–1326, 2012, doi: 10.1109/tia.2012.2199450.

[34] M. J. Kamper, R.-J. Wang, and F. G. Rossouw, "Analysis and Performance Evaluation of Axial Flux Air-Cored Stator Permanent Magnet Machine with Concentrated Coils," in *2007 IEEE International Electric Machines and Drives Conference: IEMDC] ; Antalya, Turkey, 3 - 5 May 2007*, Antalya, Turkey, 2007, pp. 13–20.

[35] F. Marignetti, G. Volpe, S. M. Mirimani, and C. Cecati, "Electromagnetic Design and Modeling of a Two-Phase Axial-Flux

Printed Circuit Board Motor," *IEEE Trans. Ind. Electron.*, vol. 65, no. 1, pp. 67–76, 2018, doi: 10.1109/TIE.2017.2716865.

[36] P. Jin *et al.*, "3-D Analytical Magnetic Field Analysis of Axial Flux Permanent-Magnet Machine," *IEEE Trans. Magn.*, vol. 50, no. 11, pp. 1–4, 2014, doi: 10.1109/tmag.2014.2323573.

[37] P. Jin, Y. Yuan, Q. Xu, S. Fang, H. Lin, and S. L. Ho, "Analysis of Axial-Flux Halbach Permanent-Magnet Machine," *IEEE Trans. Magn.*, vol. 51, no. 11, pp. 1–4, 2015, doi: 10.1109/TMAG.2015.2449352.

[38] O. Maloberti *et al.*, "3-D–2-D Dynamic Magnetic Modeling of an Axial Flux Permanent Magnet Motor With Soft Magnetic Composites for Hybrid Electric Vehicles," *IEEE Trans. Magn.*, vol. 50, no. 6, pp. 1–11, 2014, doi: 10.1109/TMAG.2014.2300152.

[39] J. Hou, W. Geng, Q. Li, and Z. Zhang, "3-D Equivalent Magnetic Network Modeling and FEA Verification of a Novel Axial-Flux Hybrid-Excitation In-wheel Motor," *IEEE Trans. Magn.*, vol. 57, no. 7, pp. 1–12, 2021, doi: 10.1109/TMAG.2021.3081830.

[40] M. Polat, A. Yildiz, and R. Akinci, "Performance Analysis and Reduction of Torque Ripple of Axial Flux Permanent Magnet Synchronous Motor Manufactured for Electric Vehicles," *IEEE Trans. Magn.*, vol. 57, no. 7, pp. 1–9, 2021, doi: 10.1109/TMAG.2021.3078648.

[41] J. Li, Y. Lu, Y.-H. Cho, and R. Qu, "Design, Analysis, and Prototyping of a Water-Cooled Axial-Flux Permanent-Magnet Machine for Large-Power Direct-Driven Applications," *IEEE Trans. on Ind. Applicat.*, vol. 55, no. 4, pp. 3555–3565, 2019, doi: 10.1109/TIA.2019.2907890.

[42] A. Schäfer *et al.*, "Design concept of a repairable YASA axial flux machine with a hybrid cooling system," in *12th International Conference on Power Electronics, Machines and Drives (PEMD 2023)*, Brussels, Belgium, 2023, pp. 119–128.

[43] W. Deng and S. Zuo, "Analytical Modeling of the Electromagnetic Vibration and Noise for an External-Rotor Axial-Flux in-Wheel Motor," *IEEE Trans. Ind. Electron.*, vol. 65, no. 3, pp. 1991–2000, 2018, doi: 10.1109/tie.2017.2736487.

[44] P. Kotter, D. Morisco, M. Boesing, O. Zirn, and K. Wegener, "Noise-Vibration-Harshness-Modeling and Analysis of a Permanent-Magnetic Disc Rotor Axial-Flux Electric Motor," *IEEE Trans. Magn.*, vol. 54, no. 3, pp. 1–4, 2018, doi: 10.1109/TMAG.2017.2759244.

[45] G. Bertotti, "General properties of power losses in soft ferromagnetic materials," *IEEE Trans. Magn.*, vol. 24, no. 1, pp. 621–630, 1988, doi: 10.1109/20.43994.

[46] C. Steinmetz, "On the law of hysteresis," *Proc. IEEE*, vol. 72, no. 2, pp. 197–221, 1984, doi: 10.1109/PROC.1984.12842.

[47] R. Nasiri-Zarandi and M. Mirsalim, "Finite Element Analysis of an Axial Flux Hysteresis Motor Based on Complex Permeability Concept Considering the Saturation of the Hysteresis Loop," *IEEE Trans. on Ind. Applicat.*, p. 1, 2015, doi: 10.1109/TIA.2015.2493059.

[48] N. Li, J. Zhu, M. Lin, G. Yang, Y. Kong, and L. Hao, "Analysis of Axial Field Flux-Switching Memory Machine Based on 3-D Magnetic Equivalent Circuit Network Considering Magnetic Hysteresis," *IEEE Trans. Magn.*, vol. 55, no. 6, pp. 1–4, 2019, doi: 10.1109/TMAG.2019.2900368.

[49] N. Taran, D. Klink, G. Heins, V. Rallabandi, D. Patterson, and D. M. Ionel, "A Comparative Study of Yokeless and Segmented Armature Versus Single Sided Axial Flux PM Machine Topologies for Electric Traction," *IEEE Trans. on Ind. Applicat.*, vol. 58, no. 1, pp. 325–335, 2022, doi: 10.1109/tia.2021.3131427.

[50] N. Aliyu, N. Ahmed, N. Stannard, and G. J. Atkinson, "AC Winding Loss Reduction in High Speed Axial Flux Permanent Magnet Machines Using a Lamination Steel Sheet," in *2019 IEEE International Electric Machines & Drives Conference (IEMDC)*, San Diego, CA, USA, 2019, pp. 1053–1060.

[51] T. Xiao, J. Li, K. Yang, J. Lai, and Y. Lu, "Study on AC Copper Losses in an Air-Cored Axial Flux Permanent Magnet Electrical Machine With Flat Wires," *IEEE Trans. Ind. Electron.*, vol. 69, no. 12, pp. 13255–13264, 2022, doi: 10.1109/TIE.2022.3144589.

[52] T. Li, Y. Zhang, Y. Liang, Q. Ai, and H. Dou, "Multiphysics Analysis of an Axial-Flux In-Wheel Motor With an Amorphous Alloy Stator," *IEEE Access*, vol. 8, pp. 27414–27425, 2020, doi: 10.1109/ACCESS.2020.2972017.

[53] H. Vansompel, P. Sergeant, and L. Dupre, "Effect of segmentation on eddy-current loss in permanent-magnets of axial-flux PM machines using a multilayer-2D — 2D coupled model," in *2012 XXth International Conference on Electrical Machines (ICEM 2012): Marseille, France, 2 - 5 September 2012 ; [proceedings*, Marseille, France, 2012, pp. 228–232.

[54] R. Benlamine, F. Dubas, S.-A. Randi, D. Lhotellier, and C. Espanet, "3-D Numerical Hybrid Method for PM Eddy-Current Losses Calculation: Application to Axial-Flux PMSMs," *IEEE Trans. Magn.*, vol. 51, no. 7, pp. 1–10, 2015, doi: 10.1109/TMAG.2015.2405053.

[55] A. Hemeida and P. Sergeant, "Analytical modeling of eddy current losses in Axial Flux PMSM using resistance network," in *2014 International Conference on Electrical Machines (ICEM)*, Berlin, Germany, Sep. 2014 - Sep. 2014, pp. 2688–2694.

[56] K.-H. Kim and D.-K. Woo, "Novel Quasi-Three-Dimensional Modeling of Axial Flux In-Wheel Motor With Permanent Magnet Skew," *IEEE Access*, vol. 10, pp. 98842–98854, 2022, doi: 10.1109/ACCESS.2022.3206774.

[57] H. Wei *et al.*, "Modeling of an Axial Field Machine (AFM) With Superconducting Windings," *IEEE Trans. Appl. Supercond.*, vol. 32, no. 4, pp. 1–5, 2022, doi: 10.1109/TASC.2022.3145295.

[58] B. Guo, Y. Huang, F. Peng, J. Dong, and Y. Li, "Analytical Modeling of Misalignment in Axial Flux Permanent Magnet Machine," *IEEE Trans. Ind. Electron.*, vol. 67, no. 6, pp. 4433–4443, 2020, doi: 10.1109/tie.2019.2924607.

[59] R. Benlamine, F. Dubas, S.-A. Randi, D. Lhotellier, and C. Espanet, "Modeling of an axial-flux interior PMs machine for an automotive application using magnetic equivalent circuit," in *2015 18th International Conference on Electrical Machines and Systems (ICEMS): 25-28 October 2015, Pattaya City, Thailand*, Pattaya, Thailand, 2015, pp. 1266–1271.

[60] Y. Huang, B. Ge, J. Dong, H. Lin, J. Zhu, and Y. Guo, "3-D Analytical Modeling of No-Load Magnetic Field of Ironless Axial Flux Permanent Magnet Machine," *IEEE Trans. Magn.*, vol. 48, no. 11, pp. 2929–2932, 2012, doi: 10.1109/TMAG.2012.2194699.

[61] M. J. Kamper, R.-J. Wang, and F. G. Rossouw, "Analysis and Performance of Axial Flux Permanent-Magnet Machine With Air-Cored Nonoverlapping Concentrated Stator Windings," *IEEE Trans. on Ind. Applicat.*, vol. 44, no. 5, pp. 1495–1504, 2008, doi: 10.1109/TIA.2008.2002183.

[62] T. Zou, D. Li, R. Qu, J. Li, and D. Jiang, "Analysis of a Dual-Rotor, Toroidal-Winding, Axial-Flux Vernier Permanent Magnet Machine," *IEEE Trans. on Ind. Applicat.*, vol. 53, no. 3, pp. 1920–1930, 2017, doi: 10.1109/TIA.2017.2657493.

[63] H. Vansompel, P. Sergeant, and L. Dupre, "A Multilayer 2-D–2-D Coupled Model for Eddy Current Calculation in the Rotor of an Axial-Flux PM Machine," *IEEE Trans. Energy Convers.*, vol. 27, no. 3, pp. 784–791, 2012, doi: 10.1109/TEC.2012.2192737.

[64] Q. Wang, F. Zhao, and K. Yang, "Analysis and Optimization of the Axial Electromagnetic Force for an Axial-Flux Permanent Magnet Vernier Machine," *IEEE Trans. Magn.*, vol. 57, no. 2, pp. 1–5, 2021, doi: 10.1109/TMAG.2020.3005216.

[65] K. Abbaszadeh and A. Rahimi, "Analytical Quasi 3D Modeling of an Axial Flux PM Motor with Static Eccentricity Fault," *Scientia Iranica*, vol. 22, no. 6, pp. 2482–2491, 2015. [Online]. Available: https://scientiairanica.sharif.edu/article_3798.html

[66] Z. Frank and J. Laksar, "Analytical Design of Coreless Axial-Flux Permanent Magnet Machine With Planar Coils," *IEEE Trans. Energy Convers.*, vol. 36, no. 3, pp. 2348–2357, 2021, doi: 10.1109/TEC.2021.3050502.

[67] Y. N. Zhilichev, "Calculation of 3D magnetic field of disk-type micromotors by integral transformation method," *IEEE Trans. Magn.*, vol. 32, no. 1, pp. 248–253, 1996, doi: 10.1109/20.477578.

[68] Y. Zhilichev, "Three-dimensional analytic model of permanent magnet axial flux machine," *IEEE Trans. Magn.*, vol. 34, no. 6, pp. 3897–3901, 1998, doi: 10.1109/20.728300.

[69] Z. Q. Zhu and D. Howe, "Analytical prediction of the cogging torque in radial-field permanent magnet brushless motors," *IEEE Trans. Magn.*, vol. 28, no. 2, pp. 1371–1374, 1992, doi: 10.1109/20.123947.

[70] A. Dwivedi, S. k. Singh, and R. K. Srivastava, "Analysis and Performance Evaluation of Axial Flux Permanent Magnet Motors," *IEEE Trans. on Ind. Applicat.*, vol. 54, no. 2, pp. 1765–1772, 2018, doi: 10.1109/TIA.2017.2776210.

[71] S.-Y. Sung, J.-H. Jeong, Y.-S. Park, J.-Y. Choi, and S.-M. Jang, "Improved Analytical Modeling of Axial Flux Machine With a Double-Sided Permanent Magnet Rotor and Slotless Stator Based on an Analytical Method," *IEEE Trans. Magn.*, vol. 48, no. 11, pp. 2945–2948, 2012, doi: 10.1109/tmag.2012.2203112.

[72] J. Azzouzi, G. Barakat, and B. Dakyo, "Quasi-3-D Analytical Modeling of the Magnetic Field of an Axial Flux Permanent-Magnet Synchronous Machine," *IEEE Trans. Energy Convers.*, vol. 20, no. 4, pp. 746–752, 2005, doi: 10.1109/tec.2005.845538.

[73] H. Zhao, K. T. Chau, T. Yang, Z. Song, and C. Liu, "A Novel Quasi-3D Analytical Model for Axial Flux Motors Considering Magnetic Saturation," *IEEE Trans. Energy Convers.*, vol. 37, no. 2, pp. 1358–1368, 2022, doi: 10.1109/TEC.2021.3132618.

[74] N. F. Lombard and M. J. Kamper, "Analysis and performance of an ironless stator axial flux PM machine," *IEEE Trans. Energy Convers.*, vol. 14, no. 4, pp. 1051–1056, 1999, doi: 10.1109/60.815027.

[75] T. D. Nguyen, K.-J. Tseng, S. Zhang, and H. T. Nguyen, "A Novel Axial Flux Permanent-Magnet Machine for Flywheel Energy Storage System: Design and Analysis," *IEEE Trans. Ind. Electron.*, vol. 58, no. 9, pp. 3784–3794, 2011, doi: 10.1109/tie.2010.2089939.

[76] P. Kurronen and J. Pyrhönen, "Analytic calculation of axial-flux permanent-magnet motor torque," *IET Electric Power Applications*, vol. 1, no. 1, p. 59, 2007, doi: 10.1049/iet-epa:20060093.

[77] P. Kurronen, *Torque vibration model of axial-flux surface-mounted permanent magnet synchronous machine*. Zugl.: Lappeenranta, Univ. of Technology, Diss., 2003. Lappeenranta: Lappeenrannan Teknillinen Yliopisto, 2003.

[78] B.-O. Tak and J.-S. Ro, "Analysis and Design of an Axial Flux Permanent Magnet Motor for in-Wheel System Using a Novel Analytical Method Combined With a Numerical Method," *IEEE Access*, vol. 8, pp. 203994–204011, 2020, doi: 10.1109/ACCESS.2020.3036666.

[79] W. Tong, S. Wang, S. Dai, S. Wu, and R. Tang, "A Quasi-Three-Dimensional Magnetic Equivalent Circuit Model of a Double-Sided Axial Flux Permanent Magnet Machine Considering Local Saturation," *IEEE Trans. Energy Convers.*, vol. 33, no. 4, pp. 2163–2173, 2018, doi: 10.1109/TEC.2018.2853265.

[80] Y. Yoshida, K. Nakamura, and O. Ichinokura, "A Method for Calculating Eddy Current Loss Distribution Based on Reluctance Network Analysis," *IEEE Trans. Magn.*, vol. 47, no. 10, pp. 4155–4158, 2011, doi: 10.1109/TMAG.2011.2156397.

[81] A. Hemeida, P. Sergeant, and H. Vansompel, "Comparison of Methods for Permanent Magnet Eddy-Current Loss Computations With and Without Reaction Field Considerations in Axial Flux PMSM," *IEEE Trans. Magn.*, vol. 51, no. 9, pp. 1–11, 2015, doi: 10.1109/TMAG.2015.2431222.

[82] S. Asfirane *et al.*, "Scalar Magnetic Potential Interpolation for Non-Conformal Meshing in Mesh-Based Generated Reluctance Networks," *IEEE Trans. Magn.*, vol. 55, no. 7, pp. 1–8, 2019, doi: 10.1109/TMAG.2019.2899820.

[83] C. Bruzzese, D. Zito, and A. Tessarolo, "Finite reluctance approach: A systematic method for the construction of magnetic network-based dynamic models of electrical machines," in *From research to industry: the need for a more effective technology transfer (AEIT 2014): 2014 AEIT annual conference : Trieste, Italy, 18 - 19 September 2014*, Trieste, 2014, pp. 1–6.

[84] P. R. Upadhyay and K. R. Rajagopal, "A novel Integral-force technique for the analysis of an axial-field permanent-magnet brushless DC motor using FE method," *IEEE Trans. Magn.*, vol. 41, no. 10, pp. 3958–3960, 2005, doi: 10.1109/TMAG.2005.854979.

[85] M. Gulec and M. Aydin, "Implementation of different 2D finite element modelling approaches in axial flux permanent magnet disc machines," *IET Electric Power Applications*, vol. 12, no. 2, pp. 195–202, 2018, doi: 10.1049/iet-epa.2017.0434.

[86] H. Tiegna, Y. Amara, and G. Barakat, "A New Quasi-3-D Analytical Model of Axial Flux Permanent Magnet Machines," *IEEE Trans. Magn.*, vol. 50, no. 2, pp. 817–820, 2014, doi: 10.1109/TMAG.2013.2285739.

[87] VEPCO Technologies, *MotorXP-AFM: Design and Analysis of Axial Flux Machines with Permanent Magnets.* [Online]. Available: https://motorxp.com/wp-content/uploads/MotorXP-AFM_brochure.pdf (accessed: Apr. 5 2024).

[88] J. D'Angelo, M. Chari, and P. Campbell, "Three-Dimensional Finite Element Solution for a Permanent Magnet Axial-Field Machine," *IEEE Trans. on Power Apparatus and Syst.*, PAS-102, no. 1, pp. 83–90, 1983, doi: 10.1109/TPAS.1983.318001.

[89] F. Locment, E. Semail, and F. Piriou, "Design and study of a multiphase axial-flux machine," *IEEE Trans. Magn.*, vol. 42, no. 4, pp. 1427–1430, 2006, doi: 10.1109/tmag.2006.872418.

[90] E. Ajily, K. Abbaszadeh, and M. Ardebili, "Three-Dimensional Field Reconstruction Method for Modeling Axial Flux Permanent Magnet Machines," *IEEE Trans. Energy Convers.*, vol. 30, no. 1, pp. 199–207, 2015, doi: 10.1109/TEC.2014.2353299.

[91] H.-J. Park, H.-K. Jung, S.-Y. Jung, Y.-H. Chae, and D.-K. Woo, "Field Reconstruction Method in Axial Flux Permanent Magnet Motor With Overhang Structure," *IEEE Trans. Magn.*, vol. 53, no. 6, pp. 1–4, 2017, doi: 10.1109/TMAG.2017.2653839.

[92] W. Geng and Z. Zhang, "Analysis and Implementation of New Ironless Stator Axial-Flux Permanent Magnet Machine With Concentrated Nonoverlapping Windings," *IEEE Trans. Energy Convers.*, vol. 33, no. 3, pp. 1274–1284, 2018, doi: 10.1109/TEC.2018.2799172.

[93] V. Rallabandi, N. Taran, D. M. Ionel, and J. F. Eastham, "On the feasibility of carbon nanotube windings for electrical machines — Case study for a coreless axial flux motor," in *ECCE 2016: IEEE Energy Conversion Congress & Expo : Sept. 18-22, Milwaukee, WI : proceedings*, Milwaukee, WI, USA, 2016, pp. 1–7.

[94] S. ARSLAN, E. KURT, O. Akizu, and J. M. LOPEZ-GUEDE, "Design optimization study of a torus type axial flux machine," *Journal of Energy Systems*, vol. 2, no. 2, pp. 43–56, 2018, doi: 10.30521/jes.408179.

[95] J.-Y. Lee, G.-D. Nam, I.-K. Yu, and M. Park, "Design and Characteristic Analysis of an Axial Flux High-Temperature Superconducting Motor for Aircraft Propulsion," *Materials (Basel, Switzerland)*, vol. 16, no. 9, 2023, doi: 10.3390/ma16093587.

[96] Y. Wang, M. Chen, T. W. Ching, and K. T. Chau, "Design and Analysis of a New HTS Axial-Field Flux-Switching Machine," *IEEE Trans. Appl. Supercond.*, vol. 25, no. 3, pp. 1–5, 2015, doi: 10.1109/TASC.2014.2366465.

[97] C.-W. Kim, G.-H. Jang, J.-M. Kim, J.-H. Ahn, C.-H. Baek, and J.-Y. Choi, "Comparison of Axial Flux Permanent Magnet Synchronous Machines With Electrical Steel Core and Soft Magnetic Composite Core," *IEEE Trans. Magn.*, vol. 53, no. 11, pp. 1–4, 2017, doi: 10.1109/TMAG.2017.2701792.

[98] S. H. Rhyu, S. Khaliq, R. E. Kim, and K. D. Lee, "Design and analysis of axial flux permanent magnet motor for electric bicycles with hybrid stator core," in *2017 20th International Conference on Electrical Machines and Systems (ICEMS): 11-14 Aug. 2017*, Sydney, Australia, 2017, pp. 1–6.

[99] F. N. Nishanth, A. D. Goodall, I. Todd, and E. L. Severson, "Characterization of an Axial Flux Machine With an Additively Manufactured Stator," *IEEE Trans. Energy Convers.*, vol. 38, no. 4, pp. 2717–2729, 2023, doi: 10.1109/TEC.2023.3285539.